2023 IEEE International Conference on Robotics and Automation (ICRA 2023)
May 29 - June 2, 2023. London, UK

MMIC-I: A Robotic Platform for Assembly Integration and Internal Locomotion through Mechanical Meta-Material Structures

Olivia Formoso[1], Greenfield Trinh[1], Damiana Catanoso[2],
In-Won Park[2], Christine Gregg[1], and Kenneth Cheung[1]

Abstract— **In-space assembly is crucial to creating large-scale space structures and enabling long term space missions. Natural limitations in the size of transportation vehicles and ISRU production facilities necessitate an additive strategy with the size of the typical structural unit being essentially fixed and inversely proportional to the final assembly size. In prior robotic and space assembly examples, reversible mechanical integration of structural modules is typically achieved with actuated alignment and fastening mechanisms onboard every structural module. Additive assembly or manufacturing planning approaches often feature a "build front" that receives new materials or parts and progresses gradually across the target geometry. The system we describe here places much of the alignment and fastener actuation systems onboard a mobile robot that can operate at a build front while companion robots (Scaling Omni-directional Lattice Locomoting Explorer, SOLL-E) provide part or material transportation. The design and evaluation of this Mobile Meta-Material Interior Co-Integrator (MMIC-I), an inchworm-style locomoting robotic assembler, is described here with an emphasis on ease of assembly and a low number of unique parts for a simple design. It is designed to assist in alignment of cuboctahedron structural unit cells with captive fasteners, defining the build front in operation. Adjacent structural unit cells are locked together with specified axial and rotational actuation of the fasteners. Hardware prototypes show that the robot is able to successfully locomote to any indexed location within a lattice structure and bolt together each set of fasteners on any interface.**

I. INTRODUCTION

Large space structures, such as stations and habitats, will enable long term missions and allow for new modes of exploration and scientific research. The current paradigm for building large structures in space is to utilize deployable mechanisms or launch separate sections to be joined through complex docking maneuvers, such as with the ISS (sometimes necessitating extravehicular personnel activities (EVA)). However, the size of these systems is limited by the capacity of the launch vehicles. Furthermore, large deployable structures require complex systems engineered for both the flight and space environments.

An alternative to deployable large scale space constructions is on-orbit or on-site assembly, in which the structure itself is a modular mechanical meta-material. Engineered modular or periodic lattice systems have many benefits with regards to both mechanical performance and manufacturability. It is accepted in the literature that architected lattice based meta-materials display desirable behaviors and performance through tuning of system geometry [1]. However, manufacturing these structures has proven to be challenging until relatively recently. Reversible mechanical assembly of this type of structural system from modular parts allows for near ideal mechanical performance [2] [3] and economical large scale manufacturing [4]. For space applications, assembly size is limited only by part supply.

For robotic assembly of such structural systems to have similar scalability, mobile robotic platforms much smaller than the structures they are assembling are needed. These robots should transport unit cells to the build front and include mobile bolting systems that connect the units together. State of the art crawling robots utilize an inchworm style motion or peristaltic worm-like gait. Singh describes a pipe-crawling robot that uses a compliant mechanism with integrated gripping pads that are radially deployed [5]. Inchworm robots developed by Lee move across a horizontal surface utilizing a sarrus linkage to constrain the motion to one degree of freedom and bidirectional compliant claws to grip to a surface [6]. Luo describes a self-deformable capsule robot that crawls by creating friction waves between the robot and the contact surface; it integrates classic and off center scissor linkages for consistent force transmission to actuate its body [7]. Kalouche developed a climbing robot designed to operate in zero gravity using pairs of long lifecycle gecko adhesive pads to walk vertically and transition between orthogonal surfaces [8].

Inchworm style robots developed by Terada suggest that genderless, rotationally symmetric connection mechanisms promote ease of robotic alignment and placement [9]. BILL-E is an inchworm style robot that locomotes along the outside of the lattice structure using passive alignment features and has the ability to transport unit cells to the build front [10]. The MOJO robot maneuvers through the internal substructure of a lattice by using its extendable arms to grab onto unit cell nodes and a rotational hip module to make turns [11]. Nigl et al. describe a hinge robot that traverses the struts of a truss structure and demonstrates manipulation and attachment of truss elements [12]. The truss climbing robot developed by Melenbrink utilizes on-board force sensing to guide build algorithms [13].

To enable the goal of autonomous assembly of high performing digital materials, a robot system must be able to locomote through the lattice in all dimensions, transport and align a unit cell to the build front, and fasten the unit cell to the existing structure. Previous mobile robots can

*This work was supported by NASA Game Changing Development (GCD) Program, Space Technology Mission Directorate

[1]Coded Structures Lab, NASA Ames Research Center, Moffett Field, CA, oliviairene.b.formoso@nasa.gov

[2]KBR, Inc., NASA Ames Research Center, Moffett Field, CA

transport and attach unit cells from the external surfaces of the structure, but do not have an integrated bolter payload for fastening unit cells together [10]. In this system, we split the split the fastening and unit cell transport capabilities between task specific robots to minimize mass transfer and avoid the energy cost of transporting a bolting module back and forth between the depot and build front [14]. The development of a crawling robot that locomotes internally through the lattice structure and joins unit cells can greatly optimize the energy efficiency of the autonomous assembly system. Increasing the number of robots and running the cargo transport and bolting tasks in parallel can further reduce assembly time. Typical multi-vehicle and multi-depot routing algorithms can be applied to these systems for robot motion planning [15], and algorithms for programmable assembly can enable orders of magnitude scalability to larger structures [16].

This paper gives an overview of the design, prototype build, and testing of MMIC-I (Mobile Metamaterial Internal Co-Integrator), an autonomous robot that crawls internally and joins structural unit cells in a lattice-based material system.

II. BACKGROUND

MMIC-I was developed in the Coded Structures Lab (CSL) within the Automated Reconfigurable Mission Adaptive Digital Assembly Systems (ARMADAS) project at NASA Ames Research Center. The ARMADAS project demonstrates autonomous robotic assembly of large structures, such as a test structure and habitat demonstration, with dimensions 1.8 m x 1.5 m x 1.5 m and 2.1 m x 2.7 m x 1.8 m, respectively. The building blocks used for this system, termed "voxels" for volumetric pixels, are cuboctahedron shaped with a characteristic pitch length of 30 cm, shown in Figure 1 [17]. They consist of six square faces with a fastener located at the corners of each face, requiring a total of 24 locked joints for a fully enclosed voxel. MMIC-I is responsible for navigating through the structure and bolting adjacent faces of a new voxel to the build front of the existing structure. The ARMADAS system is integrated with an autonomy package that determines voxel build order optimization and coordinated robot planning with interference checking. During demonstrations completed by submission of this article, MMIC-I receives commands from a central control computer and returns response packets containing acknowledgement, system status, and health information.

MMIC-I is designed to build in tandem with an external transport robot, Scaling Omnidirectional Lattice Locomoting Explorer (SOLL-E) that delivers a voxel from the depot to the build front and places the voxel in the desired position. MMIC-I completes the fine alignment of the voxel to the existing structure, and performs a series of bolting operations to connect all faces of the voxel.

The faces are connected using custom, androgynous fasteners that are pushed in the axial direction and require an applied torque of 1.5 N·m to fully lock, shown in Figure 1 [18]. This fastener design enables the usage of symmetric bolter drivers, eliminating the need to coordinate the orientation of the robot to the voxel face. These fasteners sit captive in the voxel face, so fasteners do not have to be loaded by the bolter mechanism.

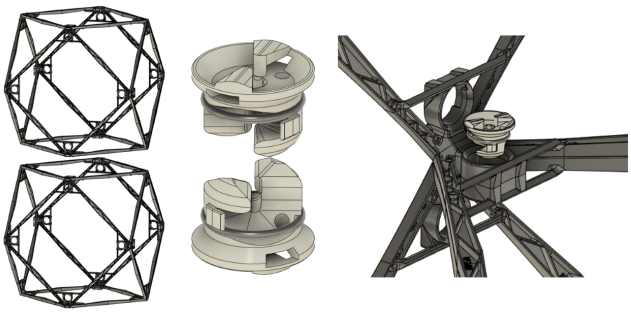

Fig. 1. The faces of two voxels (left) are connected by locking the fasteners (middle) in the vertices, and the fasteners are held captive in the fastener housing on a face (right).

III. ROBOT ARCHITECTURE

Functional requirements for MMIC-I include alignment of the voxel faces to the correct position and full engagement of the fasteners to establish robust connection with the structure. The robot has to operate fully autonomously and perform operations in a short time to increase efficiency of the overall ARMADAS robotic system. The robot must demonstrate robust performance to be able to repeatedly fulfill the requirements above.

To relax the positional requirements of the robot during fastening, passive alignment features are integrated into the mechanical design of components to account for deflections due to gravity or other structural deformations. The overall mass minimization requirement reduces stress concentrations and prevents damage to the surrounding lattice structure as it is gripped. To realize fully autonomous assembly, the robot must be able to navigate in any orthogonal direction throughout the cuboctahedral lattice substructure, and the bolter mechanism must torque the fasteners to 1.5 N·m. These values are based on the lattice structure dimensions and preload requirements of the fastener.

A. Robot Overview

The basic architecture of the robot is shown in Figure 2. Due to the periodic nature of the lattice structure, an inchworm style was chosen for MMIC-I's locomotion mechanism. MMIC-I's symmetric structure allows it to move forwards as well as backwards, through extension and contraction of the two arm modules. A hip module is located in the middle to allow turning for 3-D locomotion. The gripper module allows the robot to hold onto a voxel face between each stepping motion. The bolter modules are integrated onto the ends of the gripper module and are positioned into the bolting position when the grippers are engaged.

B. Arm Module

The arm module is responsible for the extension and contraction of the robot through a voxel. Multiple mechanisms

were investigated as candidates for the arm mechanism, including a scissor linkage, rack and pinion, and linkages with direct motor drive. A survey of commercially available actuators was conducted and their motor mass and torque capabilities were compared. The actuator and mechanism designs were assessed based on the allowable pass-through cross sectional area of the voxel and torque (2 N·m operational torque/N motor weight) needed to propel the robot locomotion and bolter module mass through the lattice. The sarrus linkage design was chosen as it allows for straight line motion and the capability to lift high loads with a large amount of travel while contracting into a compact stowed position. Initial functional testing of the robot showed small positional offsets due to gravity, and the sarrus linkage design enabled fine tuning of the robot position to account for the gravity offsets and ensure successful alignment of the gripper claws to the face.

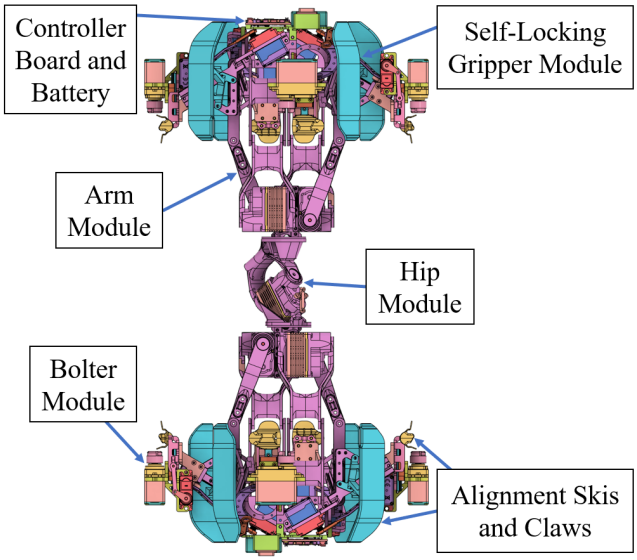

Fig. 2. The MMIC-I robot is shown in the extended position with its modules labeled.

The arm module design consists of four rotationally symmetric four bar linkages. Each individual linkage is driven by a Hitec D980 servo [19] whose form factor, operational torque of 2.15 N·m, and servo setting programmability were well suited for locomotion reliability. The servos are nested in a square configuration to allow for larger clearances between the robot and the voxel during locomotion, and the contracted and extended positions are shown in Figure 3. The free ends of the linkages are attached to the base of the gripper module. During operation, the servos rotate at the same speed simultaneously, which constrains the full mechanism to one degree of freedom.

In the fully extended position, the two arm linkages are colinear. This point was chosen to optimize the range of the servo rotation and reach a stable configuration to lock the arms in the extended position. The linkage lengths were designed to maximize the clearance between the arm motion and the voxel as the robot is locomoting through the structure, reducing the risk of the robot crashing into the structure.

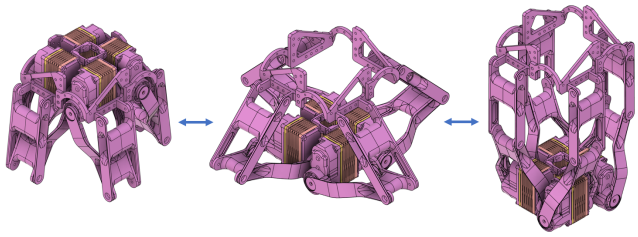

Fig. 3. The arm module is a sarrus linkage design driven by four servo motors that move simultaneously to contract (left) and extend (right) the robot in an inchworm style motion.

C. Hip Module

The hip module of the robot is designed to integrate both halves of the robot to each other through the arm modules, shown in Figure 4. It consists of a single Hitec D980 servo that rotates to the clockwise or counterclockwise position. This allows the robot to make 90° turns to enable 3-D motion through the lattice. This configuration maintains a hip rotation axis orientation that stays constantly aligned with the global orientation of the structure.

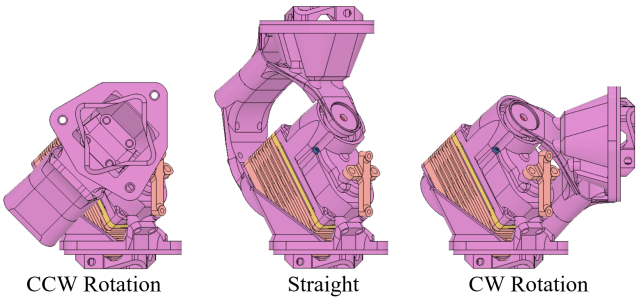

Fig. 4. The hip module has three target states: straight, rotated counterclockwise, and rotated clockwise, allowing the robot to locomote in any orthogonal direction throughout the lattice structure.

D. Gripper Module

The gripper module is designed to align to the vertices of the voxels and grip the robot in place during locomotion and bolting procedures. Shown in Figure 5, the gripper design consists of four instances of a four-bar mechanism that are arranged in a rotationally symmetric pattern around the axis of the robot, similar to how the arm module is set up. Hitec D89 servos [20] drive the linkages in a coordinated fashion, and the gripper module is able to self align the robot into the voxel face. In the extended position, the linkages slightly overextend 3° past their colinear position and the driving crank linkage is pushed against a mechanical hard stop. While under the weight of the robot, the linkages are not able to be backdriven, passively locking the gripper and robot into place on the voxel face.

The bolter modules are integrated onto the ends of the gripper mechanism. The motion of the gripper places the

bolters into position over the fastener at the vertex of each voxel face, eliminating the need for an additional mechanism to align the bolter modules. The gripper linkage is integrated onto the arm module with the gripper base. This connects the gripper servo block to the arm linkages and forms the stage that is extended and contracted by the arm modules. The gripper base is designed to connect all components while maintaining clearance for any moving parts on both the arm and gripper modules.

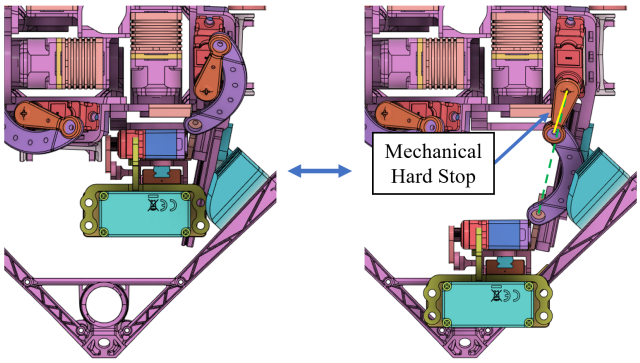

Fig. 5. The gripper module is shown in the ungripped (left) and gripped (right) position. As the gripper module extends, the linkage moves 3° past (yellow line) its colinear position (green line) and pushes the driving linkage against a hard stop, passively locking the gripper in place.

When moving through a voxel face, the clearance between the robot and the voxel is 1.5 cm. To account for small positional offsets under gravity, a set of alignment ski features are integrated onto the gripper module, which can correct up to 1.5 cm of robot deflection. The alignment skis glide along the voxel struts as MMIC-I moves through a face, increasing reliability of locomotion and avoiding interference with the structure.

The gripper linkage design is integrated with the bolter module that is outfitted with an alignment claw to aid the gripping procedure, seen in Figure 6. The claw has angled features that align the gripper module to the voxel vertex alignment bars as the gripper is fully extended. The claw features can correct positional offsets of up to 0.6 cm and slight rotational offsets the robot experiences during locomotion.

E. Bolter Module

The bolter module has a dual servo motor design shown in Figure 6. Both motors are mounted onto a linear rail, and the driver servo rotates a four bar linkage to position the fastener rotation servo at the desired height above the fastener. The fastener rotation servo directly drives the fasteners on an axis that is parallel to the linear motion driven by the driver servo. This mechanism allows the bolter to apply the required axial force and a rotational force to the fastener head to successfully lock the fasteners.

The key requirement of the bolter module is to be able to output a torque of 1.5 N·m to fully lock a fastener. A Hitec D951 servo [21] is used as the rotation actuation mechanism for turning the fasteners and has integrated safety features including a soft power up feature and overcurrent sensing. Its torque output is about 3.4 N·m which meets the operational performance needed for bolting. A Hitec D89 servo is used to provide the axial driving force of 11.6 N to push the fastener into position before turning.

The bolter module is also capable of unbolting fasteners for voxel removal. The driver bit is brought down axially onto the fastener head, and the driver bit is rotated backwards to unlock the fasteners. A catch feature is integrated onto the driver bit for pulling out the fastener. As the bolter rotates backwards, the catch moves into an undercut in the fastener head so that the fastener can be pulled up and into its disengaged position to be re-actuated and allow for structural reconfiguration.

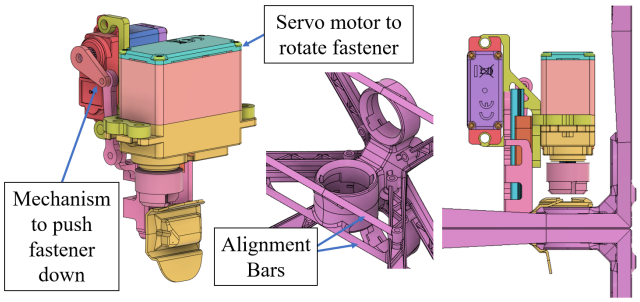

Fig. 6. The bolter module (left) has a dual servo motor design and an integrated alignment claw (center). When the grippers are fully extended, the bolters are positioned directly above the fasteners, ready to perform the bolting operation (right).

F. Avionics and Power

The robot is controlled by two custom controller boards with integrated ESP32 microcontrollers. They are mounted on each side of the robot outside the gripper module. These boards contain current sensing capabilities and an onboard IMU to sense the robot orientation as it moves throughout the lattice. All servos on a corresponding module are connected in parallel to share a ground, power, and data line. The servo positions are firmware calibrated using a calibration jig, and all servo speed settings are set to be uniform. A single signal line is used to command all four servos at the same time, ensuring the linkages move in a coordinated fashion during locomotion and reducing the complexity of the onboard controller. Automated fault sensing is integrated into the system controller, and the robot transitions into a safed positions during locomotion and bolting failures. More details on MMIC-I's firmware implementation and wireless communication are described in [22].

The robot is powered using two 11.1V 1000mAh LiPo batteries connected in parallel. The batteries, like the controller boards, are mounted on either side of the robot to maintain a balanced weight distribution across the robot. During nominal build conditions, these batteries provide up to 4 hours of continuous robot operation.

G. Robot Specifications

The overall dimensions of MMIC-I are shown in Table I. In the contracted position, it takes up a 0.2 m x 0.2 m x 0.3 m

bounding volume. The total mass is approximately 3.5 kg. This robot consists of aluminum machined parts, injection molded components, and some 3D printed features.

TABLE I
KEY ROBOT SPECIFICATIONS

Component	Characteristics
Dimension (L x W x H)	Closed, 0.2 m x 0.2 m x 0.3 m Open, 0.2 m x 0.2 m x 0.6 m
Total Mass	3.5 kg
Microcontroller	ESP32
Battery	11.1V 1000 mAh LiPo (x2)
Materials	Al, Glass fiber reinforced Nylon, PLA
Steps Completed	1106
Faces Joined	948
Fasteners Actuated	3792

Not including screws and other small connecting hardware, the total number of components on this robot is 317. However, many of the mechanisms utilize the same components. For instance, the Hitec D980 servos are used for both the hip and arm modules, the Hitec D89 servos are used for the gripper and the bolter modules, and the same size bearings are used for the arm and the gripper linkages. Taking into account the repeated instances of the mechanisms within each module brings the total number of unique part types to 40. Recurrence of same components within the robot architecture promotes ease of part replacement and enables large scale manufacturing.

IV. ROBOT OPERATION

Figure 7 shows the step by step procedure for taking a straight step, moving through a turn, and performing a bolting procedure. A complete robot step is defined as having the robot starting and ending in the contracted and fully gripped position in a voxel face.

To perform a straight vertical or horizontal step , MMIC-I contracts its front grippers and its arms extend toward the target face. Once it is fully extended, the front grippers extend to passively lock onto the target face, and the back grippers contract to unlock from the starting face. The robot arms contract to seat in the target face, and the back grippers extend to complete the step. To perform a turning step, MMIC-I follows a similar procedure as the straight step, but only extends partway to allow the hip module to rotate.

The hip module is only capable of rotating to two turning states, and in order to reach the other two adjacent faces, the robot must make an "extended turn" by first extending into a straight step and then performing a turning motion to reach the target face. We refer to the straight step, turn, and extended turn as primitive motions. By using any combination of these primitive motions, the robot is able to move in any orthogonal direction in the lattice. Fine tuning of position settings for different orientations is needed to account for deflection due to gravity, but the robot is able to fully autonomously perform its motions. On average, a straight step takes 80 seconds, a direct turn takes 115 seconds, and an extended turn takes 145 seconds to complete.

The bolting procedure is conceived to perform a translation motion along the fastener axis, and rotate the two fasteners until they interlock. The pair of bolter drivers slowly push down on the fastener heads until they are flush with the voxel nodes. The drivers then move up and repeat this downward motion to ensure the fastener is correctly seated. Servo motors on both modules rotate the driver head to fully lock the fasteners in place. Each pair of bolter modules operates sequentially, bolting one pair of fasteners at a time. MMIC-I's knowledge of a successful bolting operation is estimated by current sensing (detection of the bolter module current being above a certain given threshold). If the required torque is not reached, the robot automatically retries bolting up to two more times before triggering a fault. On average, it takes 93 seconds for all pairs of bolters to join a voxel face.

To evaluate the repeatability of the bolter, lifecycle testing was performed on the bolter module. The current sensing limit for the driving servo was set to 3A, which corresponded to the 1.5 N·m torque requirement. The bolter module ran through a normal bolting operation, and the output current of the bolter module was recorded. The current data for 1000 consecutive cycles was collected and analyzed. Figure 8 shows the data for a sample of 10 bolting cycles. The bolter performance was very stable, and the driver reached the 3 A (or 1.5 N·m) limit at every trial.

Individual test data was collected for each module functionality test. During each test, the operating current and maximum observed current on the main power line of the module was recorded, shown in Figure 8. These were compared to the maximum stall current of the servos that correspond to each module. For each module, the operating current was well under the maximum stall current of the system, which was 10 A, ensuring that the servos were able to handle the loads that the robot endures during locomotion and bolting, and confirming that there were no critical points of failure due to the motor capacity.

During the ARMADAS project ground demonstration, MMIC-I and other robots were employed to build structures consisting of hundreds of voxels. Over the course of these two builds, MMIC-I performed a total of 1106 steps and joined 948 voxel faces. The bolters actuated a total of 3792 fasteners using the current sensing protocol for confirmation of successful bolting. Operational faults and reliability metrics were recorded during the habitat demonstration. In this demo, MMIC-I performed 711 primitive motions and encountered 46 locomotion faults, resulting in a locomotion reliability of 93.5%. Twenty-seven of the locomotion faults were due to unsuccessful gripping onto the voxel face, 12 of which were remedied remotely by retrying the gripping motion. The remaining locomotion issues were caused by the locomotion overcurrent fault, which indicated that the arm module was not well seated in the contracted position or the robot was getting caught on the structure. Out of a total of 596 bolter commands that were sent during the build, there were 33 bolter faults, providing a bolter reliability of 94.5%. The bolter faults were frequently coupled with the gripper

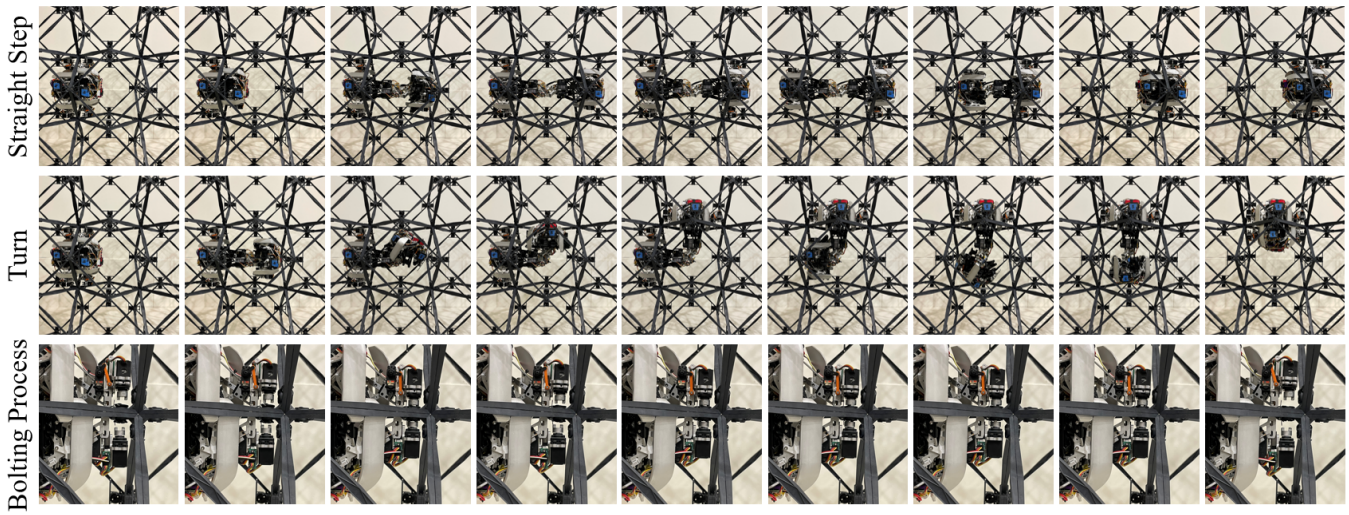

Fig. 7. MMIC-I performs a series of locomotion and bolting procedures to navigate and join voxels to an existing structure. The series of motions for a straight (horizontal or vertical) step, turn, and bolting process are visualized here.

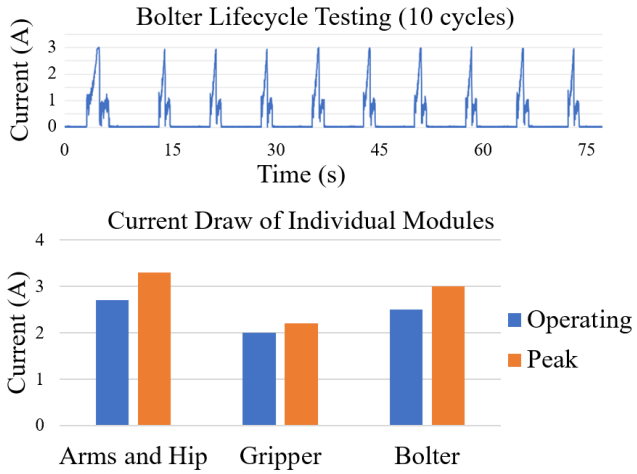

Fig. 8. The bolter operation showed high stability during bolter lifecycle testing (top) and reliably reached the required torque for locking the fastener. The current draw of the different modules were well under the stall current of the motors.

faults, indicating that the bolters were not well aligned above the fasteners in these cases. Twenty-six of these bolter faults were able to be addressed remotely by simply resending the bolter commands.

V. CONCLUSION

This paper presents the Mobile Metamaterial Internal Co-Integrator (MMIC-I) robot, an autonomous assembler that can be used for future assembly of space structures such as stations, habitats, and instrumentation. It is the one of the first examples of the family of robots that are used in mechanical metamaterial systems.

Testing and evaluation of this robot shows that it is able to successfully locomote between any two faces in the structure, perform fine positioning of a newly placed voxel, and fully engage fasteners to their locked position. The bolter mechanism is able to torque the fasteners to 1.5 N·m reliably, and also has the capability of unbolting fasteners for reconfiguration.

During an ARMADAS demonstration of autonomous assembly of a metamaterial structure, it successfully performed 1106 steps, joined 948 faces and actuated 3792 pairs of fasteners. During operation, common faults included gripping failures, arm motion failures, and unsuccessful bolting. Current sensing was integrated onto the robot to detect these faults and switch the robot to a safed mode for recovery. Future iterations of this robot can include increased sensing for more reliable locomotion and increased autonomy for fault recovery. To increase time efficiency during bolting operations, all four bolter modules can operate at the same time. Servo speeds were initially set to minimum as a safety precaution to the user and to prevent damage to the robot or structure. As testing progresses, the motion can be sped up and optimized utilizing current sensing and feedback loops in the control architecture. For future iterations of the robot, components can be injection molded or optimized to decrease cost and overall mass. This work provides a novel design of a robot that can be used for future assembly of large-scale lattice structures, and we hope that the lessons learned from this design will aid the development of future robots of this kind.

ACKNOWLEDGMENT

The authors thank the NASA Space Technology Mission Directorate's Game Changing Development program for supporting the ARMADAS project. The authors acknowledge the entire Coded Structures Lab for their hard work, resilience and dedication throughout these difficult years through the pandemic.

REFERENCES

[1] M. F. Ashby and L. J. Gibson, *Cellular solids: structure and properties*. Cambridge University Press, New York,, 1997.

[2] K. C. Cheung and N. Gershenfeld, "Reversibly assembled cellular composite materials," *science*, vol. 341, no. 6151, pp. 1219–1221, 2013.

[3] C. E. Gregg, J. H. Kim, and K. C. Cheung, "Ultra-light and scalable composite lattice materials," *Advanced Engineering Materials*, vol. 20, no. 9, p. 1800213, 2018.

[4] N. B. Cramer, J. Kim, C. Gregg, K. C. Cheung, and S. S.-M. Swei, "Modeling of tunable elastic ultralight aircraft," in *AIAA Aviation 2019 Forum*, 2019, p. 3159.

[5] P. Singh and G. Ananthasuresh, "A compact and compliant external pipe-crawling robot," *IEEE Transactions on Robotics*, vol. 29, no. 1, pp. 251–260, 2012.

[6] D. Lee, S. Kim, Y.-L. Park, and R. J. Wood, "Design of centimeter-scale inchworm robots with bidirectional claws," in *2011 IEEE International Conference on Robotics and Automation*. IEEE, 2011, pp. 3197–3204.

[7] Y. Luo, N. Zhao, K. J. Kim, J. Yi, and Y. Shen, "Inchworm locomotion mechanism inspired self-deformable capsule-like robot: Design, modeling, and experimental validation," in *2018 IEEE International Conference on Robotics and Automation (ICRA)*. IEEE, 2018, pp. 6800–6805.

[8] S. Kalouche, N. Wiltsie, H.-J. Su, and A. Parness, "Inchworm style gecko adhesive climbing robot," in *2014 IEEE/RSJ International Conference on Intelligent Robots and Systems*. IEEE, 2014, pp. 2319–2324.

[9] Y. Terada and S. Murata, "Automatic assembly system for a large-scale modular structure-hardware design of module and assembler robot," in *2004 IEEE/RSJ International Conference on Intelligent Robots and Systems (IROS)(IEEE Cat. No. 04CH37566)*, vol. 3. IEEE, 2004, pp. 2349–2355.

[10] B. Jenett and K. Cheung, "Bill-e: Robotic platform for locomotion and manipulation of lightweight space structures," in *25th AIAA/AHS Adaptive Structures Conference*, 2017, p. 1876.

[11] B. Jenett and D. Cellucci, "A mobile robot for locomotion through a 3d periodic lattice environment," in *2017 IEEE International Conference on Robotics and Automation (ICRA)*. IEEE, 2017, pp. 5474–5479.

[12] F. Nigl, S. Li, J. E. Blum, and H. Lipson, "Structure-reconfiguring robots: Autonomous truss reconfiguration and manipulation," *IEEE Robotics & Automation Magazine*, vol. 20, no. 3, pp. 60–71, 2013.

[13] N. Melenbrink, P. Michalatos, P. Kassabian, and J. Werfel, "Using local force measurements to guide construction by distributed climbing robots," in *2017 IEEE/RSJ International Conference on Intelligent Robots and Systems (IROS)*. IEEE, 2017, pp. 4333–4340.

[14] B. Bernus, G. Trinh, C. Gregg, O. Formoso, and K. Cheung, "Robotic specialization in autonomous robotic structural assembly," in *2020 IEEE Aerospace Conference*. IEEE, 2020, pp. 1–10.

[15] A. Costa, A. Abdel-Rahman, B. Jenett, N. Gershenfeld, I. Kostitsyna, and K. Cheung, "Algorithmic approaches to reconfigurable assembly systems," in *2019 IEEE Aerospace Conference*. IEEE, 2019, pp. 1–8.

[16] E. Niehs, A. Schmidt, C. Scheffer, D. E. Biediger, M. Yannuzzi, B. Jenett, A. Abdel-Rahman, K. C. Cheung, A. T. Becker, and S. P. Fekete, "Recognition and reconfiguration of lattice-based cellular structures by simple robots," in *2020 IEEE International Conference on Robotics and Automation (ICRA)*. IEEE, 2020, pp. 8252–8259.

[17] M. Ochalek, B. Jenett, O. Formoso, C. Gregg, G. Trinh, and K. Cheung, "Geometry systems for lattice-based reconfigurable space structures," in *2019 IEEE Aerospace Conference*. IEEE, 2019, pp. 1–10.

[18] O. Formoso, C. Gregg, G. Trinh, A. Rogg, and K. Cheung, "Androgynous fasteners for robotic structural assembly," in *2020 IEEE Aerospace Conference*. IEEE, 2020, pp. 1–8.

[19] "D980tw 32-bit, monster torque, titanium gear servo," https://hitecrcd.com/products/servos/digital/d-series/d980tw/product, accessed: 2022-09-01.

[20] "D89mw, 32-bit, wide voltage, metal gear servo," https://hitecrcd.com/products/servos/digital/d-series/d89mw-32bit/product, accessed: 2022-09-01.

[21] "D951tw 32-bit, metal case, high torque, titanium gear servo," https://hitecrcd.com/products/servos/d-series-servos/d951tw/product, accessed: 2022-09-01.

[22] D. Catanoso, G. Trinh, O. Formoso, I.-W. Park, T. Olatunde, C. Gregg, E. Taylor, M. Ochalek, and K. Cheung, "Rapid lightweight firmware architecture of the mobile metamaterial internal co-integrator robot," in *2023 IEEE IEEE Aerospace Conference*. IEEE, 2023.